Concentrations of inertial particles in the turbulent wake of an immobile sphere

Holger Homann and Jérémie Bec
Laboratoire J.-L. Lagrange UMR 7293, Université de Nice-Sophia Antipolis, CNRS, Observatoire de la Côte d'Azur, Bd. de l'Observatoire, 06300 Nice, France

(Dated: 28 January 2015)

Direct numerical simulations are used to study the interaction of a stream of small heavy inertial particles with the laminar and turbulent wakes of an immobile sphere facing an incompressible uniform inflow. Particles that do not collide with the obstacle but move past it, are found to form preferential concentrations both in the sphere boundary layer and in its wake. In the laminar case, the upstream diverging flow pattern is responsible for particle clustering on a cylinder that extends far downstream the sphere. The interior of this surface contains no particles and can be seen as a shadow of the large obstacle. Such concentration profiles are also present in the case of turbulent wakes but show a finite extension. The sphere shadow is followed by a region around the axis of symmetry where the concentration is higher than the average. It originates from a resonant centrifugal expulsion of particles from shed vortices. The consequence of this concentration mechanism on monodisperse inter-particle collisions is also briefly discussed. They are enhanced by both the increased concentration and the presence of large velocity differences between particles in the wake.

PACS numbers: 52.30.-q, 52.65.-y, 52.30.Cv

I. INTRODUCTION

Industrial and environmental problems often require modeling the hydrodynamic interactions between particles suspended in a turbulent flow. Sometimes it is necessary to accurately model the collision efficiencies between droplets. Instances are rain triggering by droplet coalescences in warm clouds[1] or planet formation by dust accretion in circumstellar disks.[2] In such problems one encounters different regimes: For very tiny particles associated to small values of the Reynolds number, the flow surrounding the particles is purely viscous and evolves according to the Stokes equation. When dealing with a large number of particles, this approach leads to model the collective hydrodynamic interactions in terms of *Stokesian dynamics*.[3] In turbulent carrier flows, one then generally approximates the flow as the superposition of the small-scale effects of particles and the inertial-range Navier-Stokes dynamics.[4] However, for larger particles with non-negligible Reynolds numbers, the boundary layer and wake can become rather complicated, so that for example even the drag force experienced by such particles is up to now only heuristically modeled. Therefore very little is known on the challenging problem of modeling the hydrodynamic interactions between two particles with Reynolds numbers implying that at least one particle has a turbulent wake.

In this work we focus on the asymptotic case of particles with very different sizes and investigate how a fixed sphere developing either a laminar or turbulent wake interacts with a stream of very small heavy particles. Inertia makes the trajectories of the small heavy particles deviate from fluid element trajectories and this possibly leads to particle-sphere collisions. One question is then to understand the rate at which such collisions occur and how it is accelerated or depleted as a function of the obstacle Reynolds number. This problem has important applications in the determination of dust accretion by planetesimals in early stellar systems or in the wet deposition of tiny aerosols by raindrops and is studied elsewhere. In the present work, we are concerned with the dynamics of those particles which pass the obstacle and interact with its wake. Using direct numerical simulations, we study their spatial distribution and dynamics downstream the spherical obstacle .

It is well known, that inertial particles do not exactly follow the trajectories of fluid elements and distribute with an inhomogeneous density.[5–7] Heavy particles are ejected from coherent rotating structures of the flow by centrifugal forces and concentrate in stretching regions. The creation of concentrations and voids is correlated to the local structure of the fluid velocity gradient tensor; particles concentrate in regions where it has real eigenvalues and voids appear in places where two eigenvalues are complex.[8] Figure 1 shows a snapshot from one of our simulations displaying small inertial particles in the turbulent wake of a sphere. Detached coherent vortices that are advected downstream by the mean flow eject particles and create voids. At the border of these voids, clumps of particles can be observed. These clusters trigger collisions that might be important in applications. Cloud water droplets can be this way concentrated by a falling raindrop, eventually coalesce, grow in size and influence the rain formation process.

Tang *et al.*[9] and Yang *et al.*[10] studied numerically and experimentally the influence of advected large scale structures on particle dispersion in plane mixing layers and wakes. They show that the development of highly organized patterns of inertial particles is determined by the evolution and interaction of these structures. Via the measurement of the

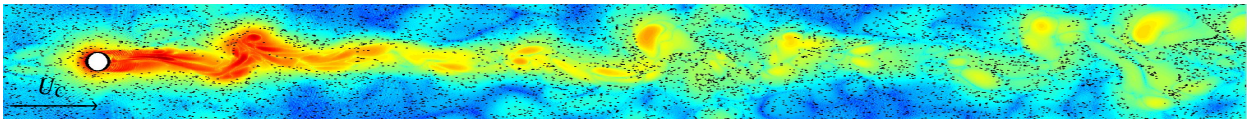

FIG. 1. Snapshot of the position of particles (with $St = \tau U_C/d = 3.2$, where U_C is the homogeneous inflow velocity and d is the diameter of the spherical obstacle) in a small slice passing through the axis of symmetry. The sphere Reynolds number is here $Re_s = U_C\, d/\nu = 400$. The background shows the values of the discriminant $\Delta = (\det[\sigma]/2)^2 - (\mathrm{tr}[\sigma^2]/6)^3$ which is positive in rotating regions and negative in stretching regions.

fractal correlation dimension they found that particles with a certain mass are the most influenced. Our work is also related to an experimental study of Jacober and Matteson.[11] In a wind tunnel they measured average concentrations of inertial particles in the turbulent wake of a sphere with Reynolds numbers ranging from 23000 to 110000. Despite the fact that these Reynolds numbers are out of reach by direct numerical simulations we find good qualitative agreement with their data.

This article is organized as follows. Section II gives a short description of the numerical method applied. Section III is dedicated to the mean concentrations of small particles in the turbulent wake, while Section IV presents an estimation of inter-particle collisions. Section V encompasses concluding remarks.

II. THE NUMERICAL METHOD

In order to conduct direct numerical simulations of a three-dimensional hydrodynamic flow around a spherical object with no-slip boundary conditions at its surface, we use a combination of a standard pseudo-Fourier-spectral method with a penalty method.[12] More precisely, we solve the incompressible Navier-Stokes equations

$$\partial_t \boldsymbol{u} + \boldsymbol{u}\cdot\nabla\boldsymbol{u} = -\frac{1}{\rho_\mathrm{f}}\nabla p + \nu\nabla^2\boldsymbol{u} + \boldsymbol{f}, \quad \nabla\cdot\boldsymbol{u} = 0, \tag{1}$$

for the fluid velocity $\boldsymbol{u}$, where ρ_f is the fluid density, ν its kinematic viscosity and $\boldsymbol{f}$ a force maintaining a uniform and constant inflow. This mean flow is imposed by keeping constant the zero mode of the stream-wise component of the velocity; the mean velocity is denoted by U_C. Equation (1) is associated to the no-slip boundary condition on the surface of the large particle at rest

$$\boldsymbol{u}(\boldsymbol{x},t) = 0 \quad \text{for } |\boldsymbol{x} - \boldsymbol{X}_S| \le d/2. \tag{2}$$

Here $\boldsymbol{X}_S$ denotes the position of the particle center and d its diameter. Homogeneous inflow conditions are achieved by using again the penalty method to remove the velocity fluctuations originating from the sphere wake at the exit of the computational domain, before they are injected upstream by periodic boundary conditions. For the time integration of (1) we use a third order Runge–Kutta scheme. The grid resolution is chosen to resolve all small scales: those of the boundary layer of the sphere and all turbulent scales in the wake. Details of the method and benchmarks can be found in Homann *et al.*[12]

For the small inertial particles, we consider spherical particles with a radius a much smaller than both the viscous boundary layer and the smallest active scale of the sphere turbulent wake (the local Kolmogorov dissipative scale $\eta = (\nu^3/\epsilon)^{1/4}$, where ϵ is the local energy dissipation rate). In this limit, particles can be approximated by point particles. Further, we assume that these particles move sufficiently slowly with respect to the fluid and that their mass density ρ_p is much higher than the fluid density ρ_f. With these assumptions the dominant hydrodynamic force exerted by the fluid is a Stokes viscous drag, which is proportional to the velocity difference between the particle and the fluid flow[13,14]

$$\ddot{\boldsymbol{X}} = \frac{1}{\tau}\Big[\boldsymbol{u}(\boldsymbol{X},t) - \dot{\boldsymbol{X}}\Big], \tag{3}$$

where the dots stand for time derivatives. The quantity $\tau = 2\rho_\mathrm{p}a^2/(9\rho_\mathrm{f}\nu)$ is called the particle response time and is a measure of the particle inertia. It is the typical relaxation time of the particle velocity to that of the fluid. We also assume that the particles are sufficiently diluted to neglect any interaction among them and any back-reaction on the flow. Usually, particle inertia is measured in terms of the Stokes number $St = \tau\,/\,\tau_\mathrm{f}$ defined by non-dimensionalizing their response time by a characteristic time scale τ_f of the carrier flow. The different time scales involved here play a role depending on which aspect of the problem we are interested in. In most cases, we use $\tau_\mathrm{f} = d/U_C$, which

corresponds to expressing the particle response time in units of the time needed to be swept over a distance d by the large-scale fluid velocity U_C. Particles with small St are closely correlated to the flow and are swept around the obstacle. Large St- particles will preferentially collide with it. Only when concerned with the particle dynamics in the turbulent wake we will use $St_\eta = \tau \,/\, \tau_\mathrm{f}$ with $\tau_\mathrm{f} = \tau_\eta = (\nu/\epsilon)^{1/2}$ (the local Kolmogorov time scale).

We report results of three simulations corresponding to three different values of the obstacle Reynolds number $Re_\mathrm{s} = U_C\, d/\nu = 100$, 400, and 1000. With this choice we cover various wake types. For the smallest Re_s the wake is steady and laminar. The intermediate value is slightly above the onset of chaotic shedding of vortices and thus slightly turbulent. For $Re_\mathrm{s} = 1000$ the wake is fully turbulent. In all cases, we consider streams of heavy particles with response times τ between 0.04 and 40.96, corresponding to Stokes numbers in the range $0.05 \leq St \leq 63$. The main parameters of the simulations are summarized in Tab. I.

Re_s	U_C	d	ν	$\ell_x \times \ell_y \times \ell_z$	$N_x \times N_y \times N_z$	N_p
100	1	0.8	$8 \cdot 10^{-3}$	$2\pi \times 2\pi \times 16\pi$	$256 \times 256 \times 2048$	$\approx 10^6$
400	1	0.8	$2 \cdot 10^{-3}$	$2\pi \times 2\pi \times 16\pi$	$256 \times 256 \times 2048$	$\approx 10^6$
1000	1	0.65	$6.5 \cdot 10^{-4}$	$2\pi \times 2\pi \times 16\pi$	$512 \times 512 \times 4096$	$\approx 10^6$

TABLE I. Parameters of the numerical simulations. $Re_\mathrm{s} = U_C\, d/\nu$: Reynolds number of the obstacle, U_C: inflow velocity, d: diameter of the spherical obstacle, ν: kinematic viscosity, ℓ_x, ℓ_y and ℓ_z: edge lengths of the computational domain (z being in the direction of the mean flow), N_x, N_y, and N_z: number of collocation points in the respective directions, N_p: number of small particles.

The simulations are set up in the following way. First, we integrate the Navier-Stokes equations (1) with a sphere located at $\boldsymbol{X}_S = (\pi, \pi, 2\,\pi)$ while imposing a homogeneous inflow with $U_c = 1$ until a (statistically) stationary state is reached. We then inject a stream of inertial particles by placing randomly many particles per time step at the entrance of the domain. They are initialized with the velocity $U_C = 1$ of the fluid. During the simulation we remove all the particles that are touching the sphere or reaching the end of the computational domain. On average the domain is filled with approximately one million particles. The fluid and particle trajectories are then stored and analyzed during four times the time needed for the fluid to travel across the numerical domain.

III. DENSITY INHOMOGENEITIES IN THE WAKE

A. Average concentrations and voids

Small inertial particles that pass over the spherical obstacle are influenced by both its boundary layer and its wake. The rotating structures in the wake eject particles and create voids and concentrations (see again Fig. 1). The mean (temporal average) particle number density is shown in Fig. 2 for the three different Reynolds numbers we have considered. Due to the axial symmetry of the problem, we adopt a cylindrical coordinate system (r, z, ϕ) (where z is in the direction of the inflow U_C) and average over the angle ϕ. One observes regions where the particle concentration is either significantly over or under its value in the inflow stream.

Let us outline the main findings: A cylindrical region where small particles concentrate is emerging at the surface of the obstacle while a shadow with a very low concentration extends downstream. In the case of the two highest Reynolds numbers (turbulent wakes), this shadow region is drastically reduced and, moreover, another over-concentration is created further downstream. This second high-concentration region around the axis of symmetry is accompanied by a conic region of reduced concentration spreading outwards. Both the high as well as the low concentrations are more pronounced for the higher Reynolds number. For $St = 3.9$ and $Re_\mathrm{s} = 1000$, we observe for example an over-concentration in the wake that is approximately 1.5 times larger than the mean concentration.

B. Stream-wise and radial profiles

The spatial dependence of these concentrations can be seen with more details in Fig. 3 (left). Particles with a small Stokes number St only create a short shadow (a few times the obstacle diameter d for $St = 0.12$) where the concentration is significantly depleted. Rapidly, at only several diameters further downstream, the density exceeds the inflow density and reaches a maximum. Beyond this point, the over-concentration slowly reduces. This is because τ_η increases (and therefore $St_\eta = \tau/\tau_\eta$ reduces) as a function of the distance from the sphere so that small-St particles

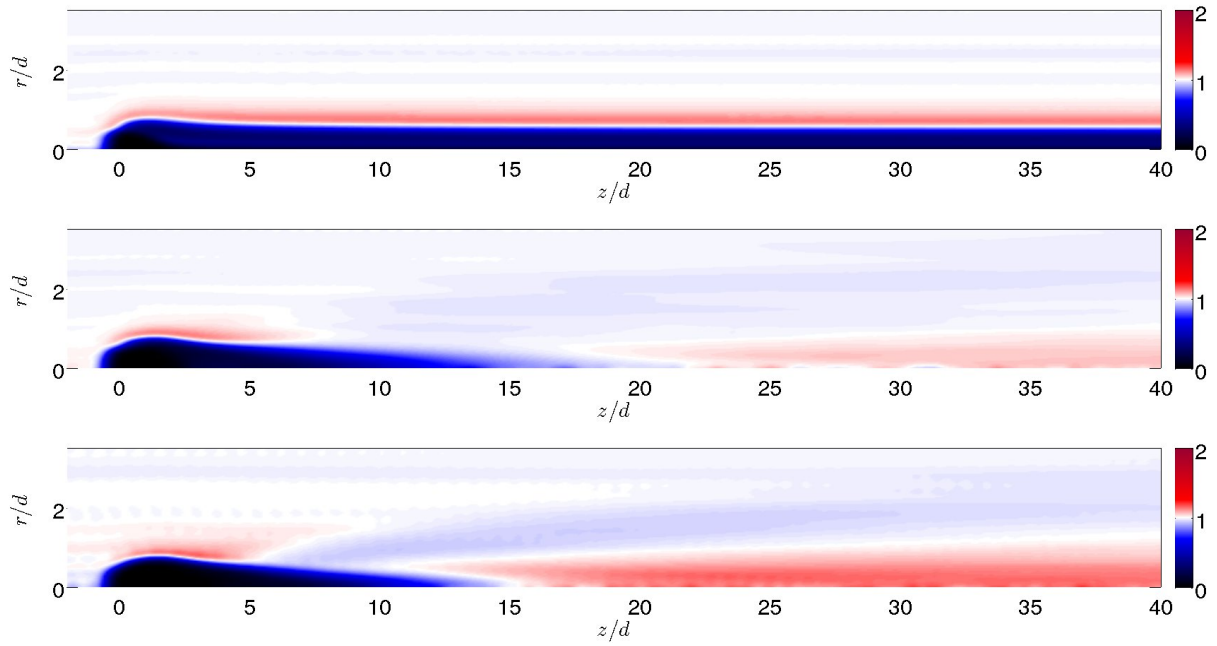

FIG. 2. Mean particle concentration for $St = 0.4$ and $Re_s = 100$ (top), $St = 0.4$ and $Re_s = 400$ (middle) and $St = 0.49$ and $Re_s = 1000$ (bottom).

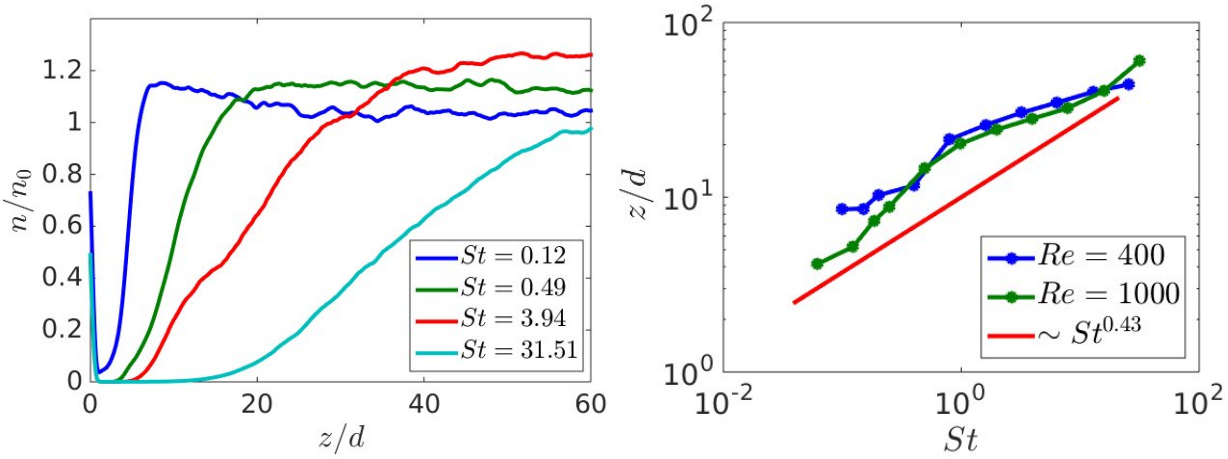

FIG. 3. Left: Mean particle concentration on the axis of symmetry as a function of the distance from the spherical obstacle for several St and $Re_s = 1000$. Data has been smoothed by a sliding window average with a window size approximately equal to d. Right: Position in the wake where the small particle density recovers the inflow density, corresponding to the transition between the shadowed region and the over-concentration.

behave more and more like tracers and stick to fluid elements. They are transported and mixed by the wake turbulent fluctuations and this evens out possible concentrations.

The density profile for particles with a larger Stokes number St is similar but shifted further downstream due to higher inertia. The concentrations might persist in the far wake as turbulence decays downstream so that heavy particles do not diffuse anymore and their density might just be advected by a quasi-uniform flow. Also, it seems that the maximum of concentration increases with St. However, these two observations cannot be unquestionably confirmed from our simulations, given the limited span in the streamwise direction. A more precise investigation of these aspects would require a much longer computational domain and is kept for a future study.

The starting point of the over-concentration region (where the particle density exceed that of the inflow) is shown in

Fig. 3 (right) as a function of St. It follows a power-law with an exponent which is close to that measured by Jacober and Matteson.[11] The decrease of the over-concentration as a function of the distance from the obstacle is reported in Fig. 4. Here, only small-St particle are considered as the position of the maximal density lies outside the domain for large St. The decay follows a power-law with an exponent close to $-2/3$.

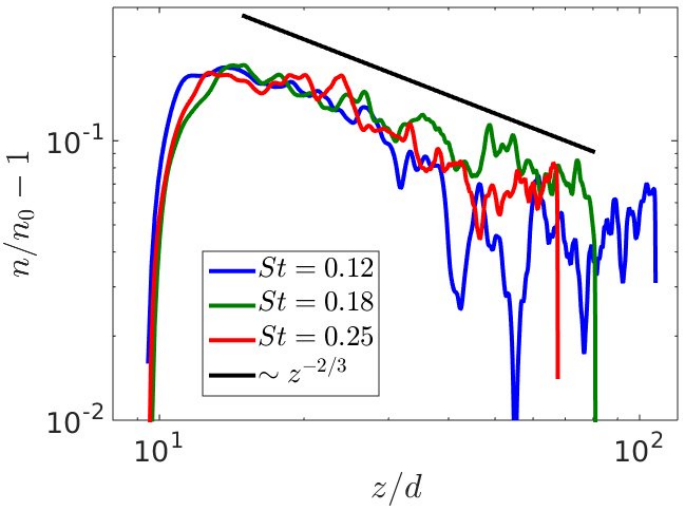

FIG. 4. Left: Mean particle concentration deficit on the axis of symmetry as a function of the distance from the obstacle center for several St. Data has been smoothed by a sliding window average with a window size of approximately d. Data is shown for $Re_s = 1000$. The black line corresponds to a decay $\propto z^{-2/3}$.

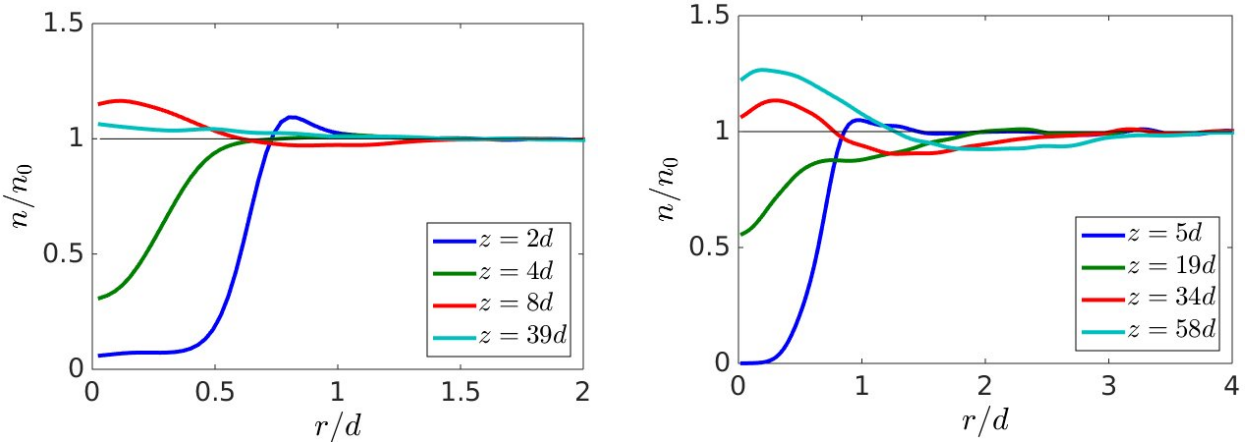

FIG. 5. Radial density profiles for various distances downstream the spherical obstacle ($Re_s = 1000$) and for $St = 0.12$ (left) and $St = 3.94$ (right)

The radial profiles of the particle density are shown in Fig. 5 for two different Stokes numbers. At small distances z from the obstacle, the high-concentration jet emerges at a radial distance $r \approx d$ from the axis of symmetry. Further downstream, the transition from regions of reduced to increased particle concentrations are also situated at $r \approx d$.

C. Concentration mechanisms

For all Reynolds numbers of the spherical obstacle, a high-concentration cylindrical jet of particles emerges directly from the surface of the sphere. The reason for this is the converging flow in front of the obstacle (see the sketch in Fig. 6). Particle trajectories that start upstream at locations close to the axis of symmetry (small r's) come close to

those starting with a larger r. This is due to reduced accelerations of the inertial particles compared to fluid elements. The observed number densities in the jet region decrease with increasing Stokes number St. This is because the collision rate of small particles with the sphere increases with St. The particles which have collided are removed from the flow and are thus missing downstream and in the jet region.

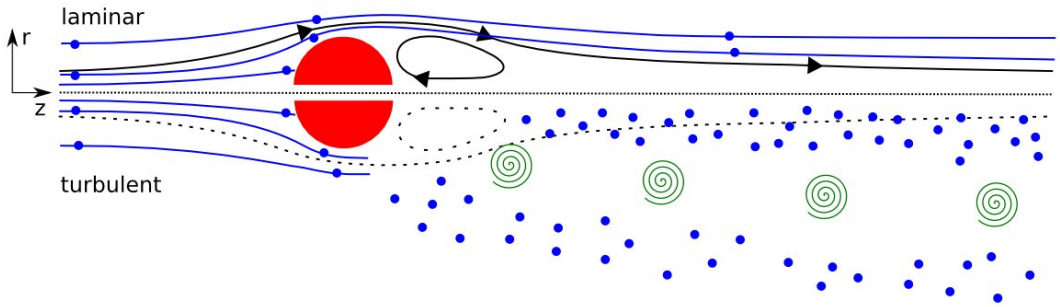

FIG. 6. Sketch showing the mechanisms leading to over- and under-concentrations of small particles in the wake of a spherical obstacle (red half-disk). The upper half shows the situation for laminar wakes while the lower part relates to turbulent wakes. Streamlines are shown in black. In the case of a turbulent wake, the stream lines of the mean flow are shown as dashed lines. Blue lines correspond to trajectories of heavy particles. In the turbulent wake particle positions are indicated by blue points. Green spirals sketch the position and rotation of detached vortices.

The low-concentration shadow behind the obstacle originates from the fact that the dynamics of inertial particles lies behind that of the fluid. Fluid streamlines converge downstream the recirculation region but inertial particles overshoot. The resulting shadow persists far away in the wake (in the laminar case), because of the turbulent decay downstream and the associated decrease of the fluid radial acceleration. Particles get less and less driven toward the center axis of symmetry.

How can one understand the emergence of the over-concentration regions in the far turbulent wakes? Jacober and Matteson[11] suggested that they originate from the jet region that is drawn around the sphere and collapses behind it. However, if this was the case, a laminar wake would also produce similar concentrations and we do not observe this effect. The mean flow in the turbulent wake is not responsible for these concentrations either. We indeed integrated trajectories of inertial particles according to (3) but transported by the mean velocity field $\bar{\boldsymbol{u}}(\boldsymbol{x})$, *i.e.* the temporally averaged velocity field of the $Re_s = 400$ simulation (not shown). Up to several diameters downstream from the fixed sphere, the concentration profile is very similar to the time dependent simulations. Notably, the jet is reproduced. However, this approach does not produce the high-concentration region in the far wake.

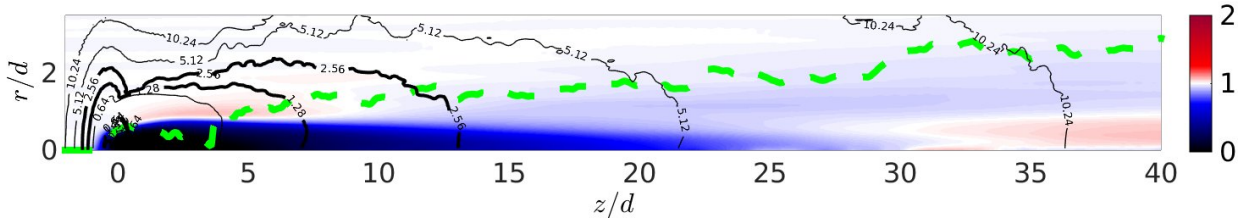

FIG. 7. Mean particle concentration in pseudo colors for $St = 1.6$ ($\tau = 1.28$) particles and $Re_s = 400$. Position of the maximal Δ as a function of the downstream distance z is shown as a dashed line. Solid black lines indicate contours of the local Kolmogorov time-scale τ_η.

We suggest that the concentration mechanism is provided by the rotating structures in the turbulent wake. Yao *et al.*[15] already observed instantaneous concentrations in a two dimensional flow past a disk and found that particles concentrate between periodically shaded vortices. Tang *et al.*[9] and Yang *et al.*[10] studied numerically and experimentally the influence of advected large scale structure on particle dispersion in plane mixing layers and wakes. They found that the development of highly organized patterns of inertial particles is determined by the evolution and interaction of these structures. Via fractal correlation dimension measurements they showed that particles with $St = 1$ are the most influenced.

In order to study with more details the effects of the wake rotating structures on particle concentrations, we com-

puted the temporally averaged Okubo–Weiss parameter Δ (defined in the caption of Fig. 1). It is a measure of the strength of rotation *vs.* stretching in the fluid velocity field. Δ is positive in regions where the velocity gradients are dominated by vorticity and negative in those where strain is dominant. In a turbulent flow, heavy inertial particles tend to move from regions where Δ is positive to those where it is negative.[7] The maximum of Δ as a function of the streamwise position is shown as the dashed line in Fig. 7. One clearly observes that it correlates well with the region of under-concentration.

Another observation is that, when the particle inertia is increased, the starting point of the concentration region is shifted downstream (compare Fig. 3). This change can be explained by the fact that particle ejection from rotating regions is the most effective for particles with a Stokes number $St_\eta = \tau/\tau_\eta$ around unity. The local Kolmogorov time scale τ_η increases downstream (see solid black contour lines in Fig. 7). Hence, the position where $St \approx 1$ shifts downstream when particle inertia increases.

IV. INTER-PARTICLE COLLISIONS

The goal of this section is to qualitatively estimate the occurrence and position of possible collisions between particles with equal inertia. We will limit the discussion to the flow $Re_s = 400$ and we focus on mean quantities, leaving the influence of fluctuations for a future work. Based on the mean pair density and on the mean approaching velocity between particles with the same Stokes number, one can estimate the collision rate is proportional to the product

$$p_c(z,r) = -\langle n_-(z,r)^2 \rangle \, \langle w_-(z,r) \rangle, \tag{4}$$

where n_-^2 is the coarse-grained pair density of approaching particles and w_- the associated mean longitudinal velocity difference. For both n_-^2 and w_-, only particles with negative longitudinal velocity differences are taken into account. Such an estimate for collision rates relies on the ghost-particle approximation[16] where possible particle encounters are counted but not performed. It relies on providing an arbitrary radius to the particles that we have here chosen to be $0.2\,d$. All the coarse-grained quantities used in (4) are thus defined for that scale. We observe from our simulations that the pair density $\langle n_-^2 \rangle$ has the same structure as the mean single particle concentrations (not shown): A high concentration jet region in the vicinity of the large sphere for particles with a small inertia and a high concentration region downstream, more pronounced for particles with a large inertia.

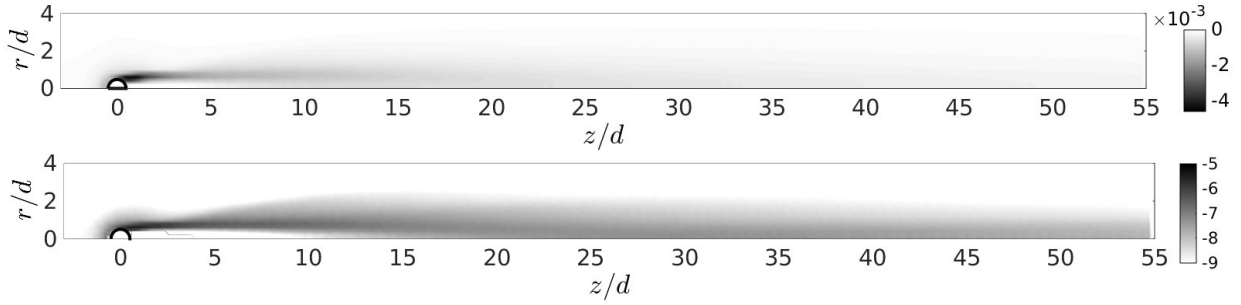

FIG. 8. Top: Average velocity difference $\langle w_-(z,r) \rangle$ of approaching particles with $St = 3.2$, coarse-grained at a scale $0.2d$. Bottom: Estimate p_c, defined in (4), for binary collisions of particles with the same $St = 3.2$. It is represented in logarithmic units in order to emphasize its variation rather than only its maximum in the jet region.

The average longitudinal velocity differences are shown in Fig. 8 (top). The highest approaching velocities are located in the jet region, where particle trajectories are compressed. In the wake region where vortices detach, one still observes some non-vanishing values of the approaching velocities, which are much less strong than in the jet region. Further in the wake, the velocity differences become weak due to the decay of turbulent fluctuations.

The estimate p_c for collision rates is shown in Fig. 8 (bottom). The jet region provides the highest probability for particle encounters. There, both the particle density as well as the particle approaching speed are enhanced. With increasing distance from the obstacle the particle collision region moves towards the axis of symmetry and the probability of collisions decreases. The dependence of the collision probability as a function of the distance from the obstacle can be seen more clearly in Fig. 9, where we show the sum of p_c over planes (r,θ) as a function of the streamwise direction z. One clearly observes that the particles with a small inertia collide preferentially in the jet

region, in the vicinity of the sphere. The collisions between particles with a larger inertia are rather enhanced in the wake. We indeed see in Fig. 9 that non-vanishing values of p_c persist at downstream distances as far as tens of the obstacle diameter.

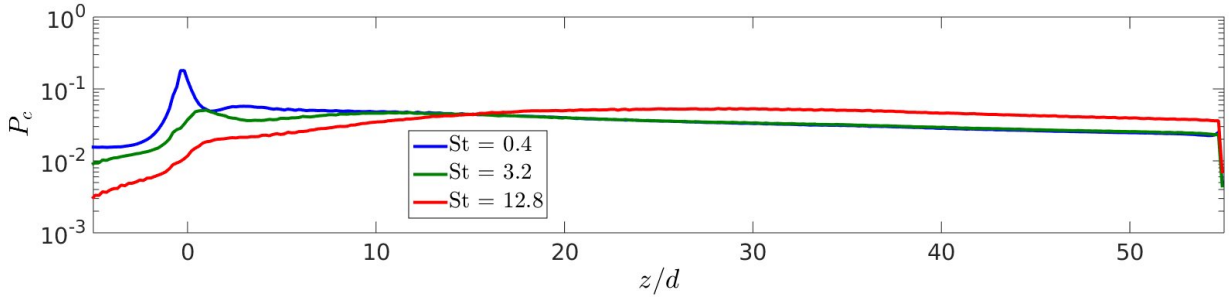

FIG. 9. Sum of p_c over planes (r, θ) in directions perpendicular to the stream, as a function of the downstream distance to the obstacle. Three different strengths of particle inertia are shown, as labeled.

V. SUMMARY AND OUTLOOK

In this work we have analyzed how a stream of inertial particles is influenced by the boundary layer and the wake of a spherical obstacle. We make use of the results of three direct numerical simulations of the incompressible Navier–Stokes equations using a combination of a Fourier-spectral method and a penalty technique. We considered three different Reynolds numbers for the sphere, $Re_s = 100$, $Re_s = 400$, and $Re_s = 1000$. The average concentration of small inertial particles shows different characteristics in the wake of the spherical obstacle, depending on the particle Stokes number St and on the sphere Reynolds number Re_s: For all Re_s we find that particles with weak or moderate inertia cluster at the outer edge of the obstacle creating a narrow cylindrical jet of particles. Behind the obstacle, inertia is responsible for the formation of a shadow where particle concentration is strongly reduced. When the wake of the obstacle is laminar, these over- and under-concentrations persist far downstream while they are rapidly dissipated by fluctuations for a turbulent wake. Moreover, we find that in the turbulent case, there is a region appearing a couple of diameters downstream the sphere where the particle concentration exceeds that in the inflow. This can be explained by resonant ejections of particles from detached and advected vortices with a local turn-over time τ_η of the order of the particle response time τ.

Estimates of the probability of collisions between identical particles show that particles with a weak inertia tend to collide in the jet region near the sphere while those with a strong inertia collide preferentially further downstream. In a future work it will be interesting to examine such collision statistics in the polydisperse case, *i.e.* between particles with different sizes and response times. We expect that in the turbulent wake the relative velocity of particles with different inertia will be larger than for particles of the same type. We also plan to take coagulation or coalescences into account and analyze how the particle size distribution is affected by the wake of the spherical obstacle and how it depends on the Reynolds number of the latter and on the downstream distance. This can have important applications, for instance in planet formation. It seems well founded to assume that large bodies, such as planetesimals or planetary embryos, will concentrate dust in their wake and will thus foster accretion and the formation of other objects.

Acknowledgments

We thank P. Tanga and T. Guillot for useful discussions. Most of the simulations were done using HPC resources from GENCI-IDRIS (Grant i2011026174). Part of them were performed on the ¢mésocentre de calcul SIGAMM¢. The research leading to these results has received funding from the Agence Nationale de la Recherche (Programme Blanc ANR-12-BS09-011-04).

[1] H. Pruppacher and J. Klett, *Microphysics of Clouds and Precipitation*. Dordrecht: Kluwer Academic, 1997.
[2] J. J. Lissauer, "Planet formation," *Annu. Rev. Astron. Astrophys.*, vol. 31, pp. 129–174, 1993.
[3] J. Brady and G. Bossis, "Stokesian dynamics," *Annual Review of Fluid Mechanics*, vol. 20, pp. 111–157, 1988.
[4] L.-P. Wang, B. Rosa, H. Gao, G. He, and G. Jin, "Turbulent collision of inertial particles: Point-particle based, hybrid simulations and beyond," *International Journal of Multiphase Flow*, vol. 35, pp. 854 – 867, 2009.

[5]K. Squires and J. Eaton, "Preferential concentration of particles by turbulence," *Phys. Fluids A*, vol. 3, pp. 1169–1178, 1991.
[6]M. Wood, W. Hwang, and K. Eaton, "Preferential concentration of particles in homogeneous and isotropic turbulence," *International Journal of Multiphase Flow*, vol. 31, pp. 1220–1230, 2005.
[7]J. Bec, L. Biferale, M. Cencini, A. Lanotte, S. Musaccio, and F. Toschi, "Heavy particle concentration in turbulence at dissipative and inertial scales," *Phys. Rev. Lett.*, no. 98, p. 84502, 2007.
[8]J. Bec, "Multifractal concentrations of inertial particles in smooth random flows," *J. Fluid Mech.*, vol. 528, pp. 255–277, 2005.
[9]L. Tang, F. Wen, Y. Yang, C. T. Crowe, J. N. Chung, and T. R. Troutt, "Selforganizing particle dispersion mechanism in a plane wake," *Physics of Fluids A: Fluid Dynamics (1989-1993)*, vol. 4, p. 2244, 1992.
[10]Y. Yang, C. Crowe, J. Chung, and T. Troutt, "Experiments on particle dispersion in a plane wake," *International Journal of Multiphase Flow*, vol. 26, pp. 1583 – 1607, 2000.
[11]D. E. Jacober and M. J. Matteson, "Particle Mixing and Diffusion in the Turbulent Wake of a Sphere Particle Mixing and Diffusion in the Turbulent Wake of a Sphere," *Aerosol Science and Technology*, no. 12, pp. 335–363, 1990.
[12]H. Homann, J.Bec, and R. Grauer, "Effect of turbulent fluctuations on the drag and lift forces on a towed sphere and its boundary layer," *J. Fluid Mech*, vol. 721, pp. 155–179, 2013.
[13]M. R. Maxey and J. Riley, "Equation of motion for a small rigid sphere in a nonuniform flow," *Phys. Fluids*, vol. 26, no. 4, p. 883, 1983.
[14]R. Gatignol, "The Faxén formulae for a rigid sphere in an unsteady non-uniform Stokes flow," *J. Méc. Théor. Appl.*, vol. 1, pp. 143–160, 1983.
[15]J. Yao, Y. Zhao, N. Li, Y. Zheng, G. Hu, J. Fan, and K. Cen, "Mechanism of Particle Transport in a Fully Developed Wake Flow," *Industrial & Engineering Chemistry Research*, pp. 10936–10948, Aug. 2012.
[16]S. Sundaram and L. R. Collins, "Collision statistics in an isotropic particle-laden turbulent suspension. Part 1. Direct numerical simulations," *J. Fluid Mech.*, vol. 335, pp. 75–109, 1997.